

JOURNAL OF THE AMERICAN CHEMICAL SOCIETY

© Copyright 1986 by the American Chemical Society

VOLUME 108, NUMBER 22

OCTOBER 29, 1986

Isomerization of Polyacetylene Films of the Shirakawa Type—Spectroscopy and Kinetics

Harry W. Gibson,[†] Samuel Kaplan,* Ralph A. Mosher, W. M. Prest, Jr., and Ronald J. Weagley

Contribution from the Webster Research Center, Xerox Corporation, Webster, New York 14580.
Received April 7, 1986

Abstract: The isomerization of Shirakawa-type polyacetylene has been examined in detail by an extensive coordinated Fourier Transform Infrared (FTIR) and ¹³C cross polarization magic angle spinning NMR (CP-MAS-NMR) study. The two techniques yield corroborative isomeric composition results. Isomerization behavior of the 740 (cis) and 1013 (trans) cm⁻¹ out-of-plane C-H deformation band positions and line shapes and ¹³C NMR line widths supports a random event mechanism rather than a nucleation type mechanism. Stochastic modeling of the 1329-cm⁻¹ cis in-plane C-H deformation band intensities suggests that the initial ~70% of the isomerization proceeds as random triad crankshaft CCC → TCT processes followed by the diffusion of trans bonds via CCT ⇌ TCC processes, which facilitate additional CCC → TCT conversions. The isomerization proceeds further by higher order crankshaft coordinated rearrangements. Even though isomerization rates vary, the same mechanisms prevail for all samples studied, independent of sample preparation, history, and isomerization temperature. Because these processes require specific sequences, there is a statistical limit. Experimentally a residual cis content of 5–7% is observed. IR and NMR data support the conclusion that isomerization is fastest in disordered regions, and it is suggested that differences in isomerization rates of materials prepared with subtle variations in synthetic procedure are due to differences in film morphology.

Polyacetylene, $-(CH=CH-)_n$, the parent member of the class of conjugated hydrocarbon polyenes, is presently the subject of intense study because insoluble free-standing films^{1,2} of the polymer can be oxidized with electron acceptors or reduced by electron donors (in processes known as p- and n-doping, respectively) to a highly conductive state.²⁻⁴ The possibility of the fabrication of lightweight, cheap, flexible electrical conductors and semiconductors suggests an exciting array of potential applications. In order to realize and generalize these possibilities, polyacetylene is being closely examined⁵ as a prototypical system to determine those molecular, electronic, and solid-state properties which produce high electrical conductivity in organic polymers in general and polyenes in particular.^{6,7}

The bonds in polyacetylene are of two types: long (single) and short (double), i.e., delocalization is incomplete.^{3,4} Were it not, polyacetylene would be electrically conductive without doping. Delocalization is incomplete because the Peierls distortion (unequal bond lengths) lowers the total energy of the polymer by reducing electron repulsions.^{3,4} There are two possible geometries about the double bonds (cis and trans) and two possible geometries about the single bonds (cisoid and transoid). Thus, a total of four possible isomeric structures exist for polyacetylene as shown in Figure 1, the cis-cisoid, which is helical, and the cis-transoid, the trans-cisoid, and the trans-transoid, which are all linear.

The isomerization of polyacetylene from the as-formed cis isomer (the cis-transoid form) to the thermodynamically more stable trans isomer is important because of its influence upon

electrical properties and from a fundamental viewpoint. A number of studies of the isomerization have been reported, including infrared,⁸⁻¹⁰ Raman¹¹⁻¹⁸ and electron spin resonance¹⁹⁻²² spec-

- (1) Ito, T.; Shirakawa, H.; Ikeda, S. *J. Polym. Sci., Polym. Chem. Ed.* **1974**, *12*, 11–20.
- (2) Gibson, H. W.; Pochan, J. M. In *Encyclopedia of Polymer Science and Engineering*; J. Wiley and Sons: New York, 1985; pp 87–130.
- (3) MacDiarmid, A. G.; Heeger, A. J. *Synth. Met.* **1980**, *1*, 101–118.
- (4) Duke, C. B.; Gibson, H. W. In *Kirk-Othmer Encyclopedia of Chemical Technology*; J. Wiley and Sons: New York, 1982; Vol. 18, pp 755–794.
- (5) Saxman, A. M.; Liepens, R.; Aldissi, M. *Prog. Polym. Sci.* **1985**, *11*, 57–89.
- (6) Naarmann, H. *Angew. Makromol. Chem.* **1982**, *109/110*, 295–338.
- (7) Gibson, H. W. In *Handbook on Conducting Polymers*; Skotheim, T., Ed.; M. Dekker: New York, 1985; pp 405–439, and other chapters therein.
- (8) Ito, T.; Shirakawa, H.; Ikeda, S. *J. Polym. Sci., Polym. Chem. Ed.* **1975**, *13*, 1943–1950.
- (9) Montaner, A.; Galtier, M.; Benoit, C.; Aldissi, M. *Solid State Commun.* **1981**, *39*, 99–101.
- (10) Jing, X.; Wu, Y.; Gong, X.; Yu, H.; Zhang, W.; Wang, F. *Makromol. Chem., Rapid Commun.* **1984**, *5*, 311–318.
- (11) Shirakawa, H.; Ito, T.; Ikeda, S. *Polym. J.* **1973**, *4*, 460–462.
- (12) Harada, I.; Tasumi, M.; Shirakawa, H.; Ikeda, S. *Chem. Lett.* **1978**, 1411–1414.
- (13) Kuzmany, H.; Imhoff, E. A.; Fitchen, D. B.; Sarhangi, A. *Mol. Cryst. Liq. Cryst.* **1981**, *77*, 197–207.
- (14) Lefrant, S.; Lichtmann, S. L.; Temkin, H.; Fitchen, D. B.; Miller, D. C.; Whitwell, G. E., II; Burlitch, J. M. *Solid State Commun.* **1979**, *29*, 191–196.
- (15) Lefrant, S. *J. Phys. (Paris) Coll. C3* **1983**, *44*, 247–254.
- (16) Bolognesi, A.; Catellani, M.; Destri, S.; Morelli, G.; Porzio, W.; Turbino, R. *Makromol. Chem., Rapid Commun.* **1983**, *4*, 403–409.
- (17) Turbino, R.; Piseri, L.; Dellepiane, G.; Piaggio, P. *J. Phys. (Paris) Coll. C3* **1983**, *44*, 329–332.
- (18) Bott, D. C.; Chai, C. K.; Gerrard, D. L.; Weatherhead, R. H.; White, D.; Williams, K. P. *J. Phys. (Paris) Coll. C3* **1983**, *44*, 45–52.

[†] Present address: Department of Chemistry, Virginia Polytechnic Institute and State University, Blacksburg, VA 24061.

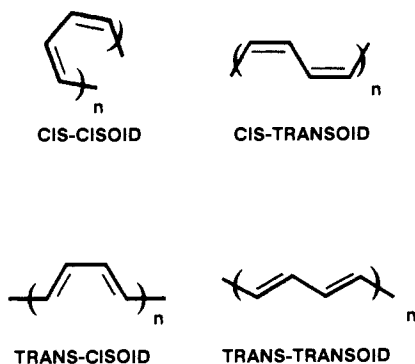


Figure 1. Isomers of polyacetylene.

Table I. Polyacetylene Films

sample no.	substrate	f_c/f_t^a	approximate ^b thickness (μm)	isomerization temp ($^\circ\text{C}$)
PAC 1	free standing		100	100
PAC 2	free standing	1.6	22	100
PAC 3	KBr disc	1.8	6	110
PAC 4	KBr disc	1.7	7	100
PAC 5	KBr disc	1.6	15	100
PAC 6	glass disc	1.5	20	100
PAC 7	KBr disc ^c	1.5	8	100
PAC 8	KBr disc	1.5	5	90
PAC 10	KBr disc	1.6	8	80
PAC 11	KBr disc	1.5	6	100
PAC 12 ^d	KBr disc	1.5	9	90/72 ^e
PAC 13 ^d	KBr disc	1.5	9	72

^aRatio of the response factors for the cis and trans out-of-plane deformation IR bands (see text). ^bThicknesses are based upon the SEM measured thickness of $\sim 6 \mu\text{m}$ for PAC 3 scaled according to the relative peak areas of the out-of-plane deformation bands for each sample. More precisely, these numbers are a measure of the amount of material in the IR beam path, i.e., thickness times density. Densities are assumed constant for simplicity. ^cPAC 7 was prepared on a KBr substrate supported by a glass disc, which was surrounded by a "pool" of toluene. ^dPAC 12 and PAC 13 are identical samples prepared together at the same time in the same reactor. ^ePAC 12 was isomerized at 90°C to 50% cis followed by 72°C to completion.

troscopies as well as an in situ kinetic analysis by synchrotron radiation to follow the evolution of the crystal structure.²³ Conventional X-ray studies have also been carried out as a function of isomeric composition.²⁴⁻²⁷ In this work we present a detailed coordinated analysis of the thermal isomerization of polyacetylene by IR and NMR spectroscopies. Some of the results have been previously communicated,²⁸⁻³¹ as have brief discussions of the physical ramifications of our conclusions regarding the molecular structure of trans polyacetylene.^{32,33}

(19) Bernier, P.; Linaya, C.; Rolland, M.; Aldissi, M. *J. Phys. Lett.* **1981**, *42*, 295-299.

(20) Rolland, M.; Bernier, P.; Lefrant, S.; Aldissi, M. *Polymer* **1980**, *21*, 1111-1112.

(21) Simonescu, C. I.; Cascaval, C.; Blascu, V.; Negulescu, I. I. *Polymer* **1982**, *23*, 1862-1863.

(22) Vansco, G.; Egyed, O.; Pekker, S.; Janossy, A. *Polymer* **1982**, *23*, 14-17.

(23) Riekell, C. *Makromol. Chem., Rapid Commun.* **1983**, *4*, 479-483.

(24) Robin, P.; Pouget, J. P.; Comes, R.; Gibson, H. W.; Epstein, A. J. *Phys. Rev. B* **1983**, *27*, 3938-3941.

(25) Robin, P.; Pouget, J. P.; Comes, R.; Gibson, H. W.; Epstein, A. J. *J. Phys. (Paris) Coll. C3* **1983**, *44*, 77-81.

(26) Ito, T.; Shirakawa, H.; Ikeda, S. *Kobunshi Ronbunshu (Engl. Ed.)* **1976**, *5*, 470-479.

(27) Perigo, G.; Lugli, G.; Pedretti, U.; Cernia, E. *J. Phys. (Paris) Coll. C3* **1983**, *44*, 93-96.

(28) Gibson, H. W.; Pochan, J. M.; Kaplan, S. *J. Am. Chem. Soc.* **1981**, *103*, 4619-4620. Infrared data in this paper are erroneous due to saturation effects.

(29) Kaplan, S.; Gibson, H. W.; Mosher, R. A.; Prest, W. M., Jr. *Proceedings, IUPAC 28th Macromolecular Symposium*, Amherst, MA, July 12-16, 1982; p 16.

(30) Gibson, H. W.; Prest, W. M., Jr.; Mosher, R. A.; Kaplan, S.; Weagley, R. J. *Polymer Prep.* **1983**, *24*, 153-154.

(31) Gibson, H. W.; Weagley, R. J.; Prest, W. M., Jr.; Mosher, R. A.; Kaplan, S. *J. Phys. Coll. C3* **1983**, *44*, 123-126.

Results and Discussion

I. Sample Preparation. Three types of samples were used in this work: (1) $\sim 100 \mu\text{m}$ thick free-standing film for NMR analysis, (2) $\sim 22 \mu\text{m}$ thick free-standing film for NMR and IR measurements, and (3) $\leq 20 \mu\text{m}$ thick films deposited on potassium bromide and glass substrates for IR studies. Table I lists the samples investigated in the current study, giving the appropriate sample designation, isomerization temperature and other features of each film. All films were synthesized with the standard Shirakawa catalyst concentration.¹² Film thickness was controlled by careful regulation of the acetylene exposure time. In order to produce $\leq 20 \mu\text{m}$ films on substrates, the acetylene was removed after only a very brief exposure. The resulting samples were of uniform thickness, as exemplified by the scanning electron micrograph in Figure 2. Subtle variations in synthetic conditions, such as catalyst concentration or acetylene exposure time, lead to polymers with different measured isomerization rates. The IR and NMR evidence presented herein suggest that these differences can be attributed to variations in sample morphology.

II. Instrumental Techniques: Calibration. The isomerization process was followed with Fourier transform infrared (FTIR) spectroscopy. The computerized aspects of FTIR enable real time monitoring of the isomerization process and facilitate detailed analysis of spectra stored in memory. ¹³C cross polarization magic angle spinning nuclear magnetic resonance spectroscopy (CP-MAS-NMR) was utilized to corroborate the FTIR calibration and to obtain additional structural information.

Figure 3 is an FTIR spectrum of a polyacetylene film containing significant amounts of cis and trans isomers. Spectral assignments for the two isomers have been made previously.^{34,35} The 740-cm^{-1} and 1013-cm^{-1} absorptions are due to C-H out-of-plane deformations of the cis and trans isomers, respectively. The 1329-cm^{-1} absorption is assigned to the cis C-H in-plane deformation and the 3011-cm^{-1} band to the trans C-H stretch. The isomerization process converts material containing a few trans bonds in a chain of predominantly cis bonds to a material with a few cis bonds in a chain of trans bonds. Figure 4 shows the evolution of these four bands with isomerization time at 100°C .

Meaningful quantitative transmission infrared analysis requires pinhole-free samples which cover the entire sample beam, and for grating instruments, the cis and trans absorbances must each be less than unity.³⁶ For the out-of-plane absorbances, the latter criterion requires polyacetylene samples whose thickness is $< 10 \mu\text{m}$. By using careful calibration methods it has been shown that the transmission FTIR method gives accurate results for absorbances as high as 1.5.³⁷ For the 20 (PAC 6) and 22 (PAC 2) μm samples, absorbances, are < 1.5 except at very high trans contents, where quantitative data become unreliable.

All isomerizations were carried out between 72 and 110°C , where cross-linking is unlikely,^{19,20} in order to ensure that the sum total of the number of cis and trans double bonds remains constant. The concentration of a chromophore is equal to the integrated absorbance, A , divided by the product of the molar absorption coefficient, ϵ , and the sample thickness (path length), b . The fibrillar (i.e., porous) nature of these films and the multicomponent nature (vide infra) of these absorptions make it more appropriate to lump these terms into effective response factors, f_c and f_t , for the cis and trans bands, respectively. Assuming that the total number of double bonds is constant, then

$$N_{\text{total}} = N_{\text{trans}} + N_{\text{cis}} = f_t A_t + f_c A_c \quad (1)$$

The ratio of response factors for cis and trans out-of-plane absorbances, f_c/f_t , can be determined from the slope of a plot of the integrated trans (1013 cm^{-1}) areas (A_t) vs. the integrated cis (740

(32) Gibson, H. W.; Weagley, R. J.; Mosher, R. A.; Kaplan, S.; Prest, W. M., Jr.; Epstein, A. J. *Phys. Rev. B* **1985**, *31*, 2338-2342.

(33) Gibson, H. W.; Weagley, R. J.; Mosher, R. A.; Kaplan, S.; Prest, W. M., Jr.; Epstein, A. J. *Mol. Cryst. Liq. Cryst.* **1985**, *117*, 315-318.

(34) Shirakawa, H.; Ikeda, S. *Polym. J.* **1971**, *2*, 231-244.

(35) Galtier, M.; Charbonnel, M.; Montaner, A.; Ribet, J. L. *Polymer* **1984**, *25*, 1253-1257.

(36) Robinson, D. Z. *Anal. Chem.* **1951**, *23*, 273-277.

(37) Mosher, R. A.; Prest, W. M., Jr., in preparation.

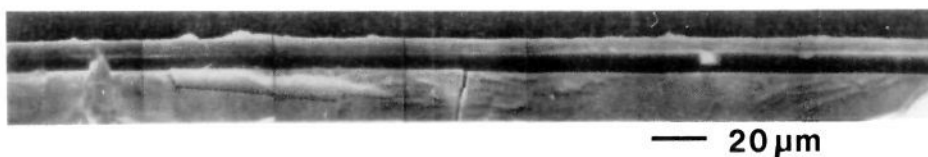


Figure 2. Scanning electron micrograph of cross section of PAC 3 polyacetylene film (gray area in middle) on KBr (gray area at bottom). The film has been lifted slightly from the substrate with a microtool.

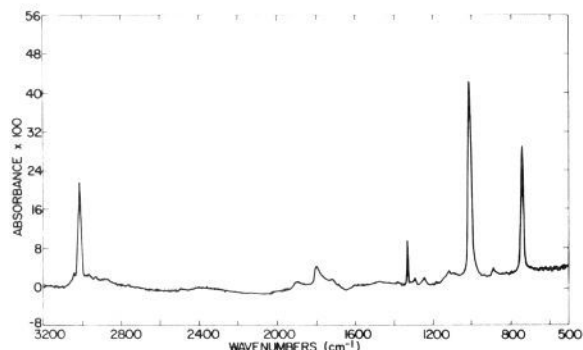


Figure 3. Fourier transform infrared (FTIR) spectrum of a polyacetylene thin film of mixed isomeric composition.

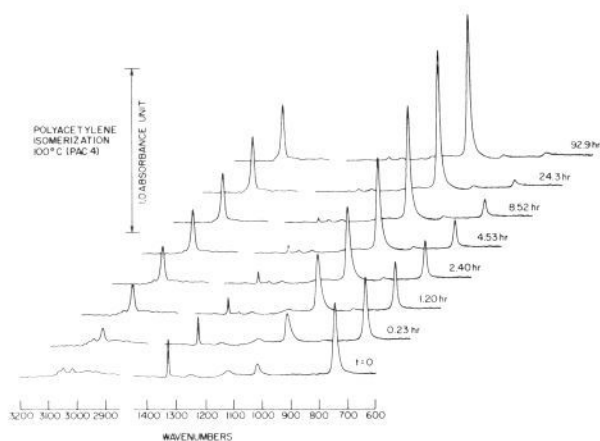


Figure 4. Evolution of FTIR spectra in the 600–1450-cm⁻¹ and 2850–3200-cm⁻¹ regions as a function of time at 100 °C.

cm⁻¹) areas (A_c). Each isomerization experiment produced from 50 to 200 individual data points. The results from five different experiments are shown in Figure 5. The linear relationship between the cis and trans band areas indicates that the response factors are constant throughout the isomerization. Deviations from linearity become pronounced for films with high absorbances (>1.5) and/or pinholes. For this reason, no IR measurements were made on films exceeding 22 μm in thickness or with pinholes. The ratio of the response factors, f_c/f_t , averaged over eleven independent isomerizations is 1.57 ± 0.20 . The fraction of cis bonds, [C], was determined by

$$[C] = \frac{(f_c/f_t)A_c}{(f_c/f_t)A_c + A_t} \quad (2)$$

using the integrated areas and the calibration factors defined by each individual experiment. The calculated cis content is insensitive to small changes in the ratio of response factors and is probably accurate to $\pm 2\%$.

In order to utilize the out-of-plane deformations to determine isomeric content, the assumption has been made that these bands represent local rather than extended modes. Furthermore, the cis and trans bands are not single modes but are superpositions of overlapping bands due to microstructural heterogeneity. For this reason it is important to use integrated intensities rather than peak heights to obtain an accurate measure of the isomeric composition. Estimates of isomeric composition using absorbances

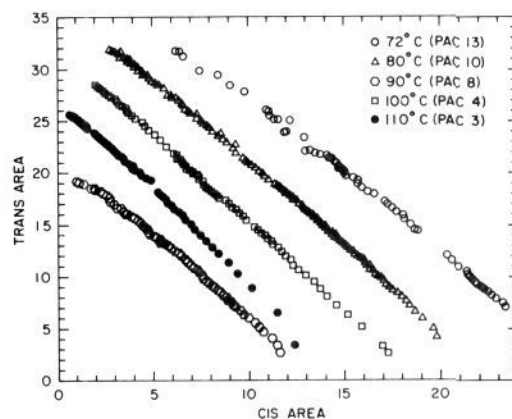


Figure 5. Integrated area of 1013 cm⁻¹ (trans) absorption vs. integrated area of 740 cm⁻¹ (cis) absorption (in arbitrary units) during isomerization at several temperatures.

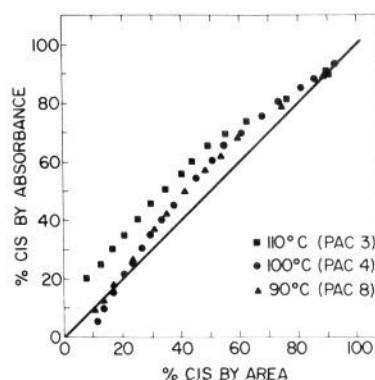


Figure 6. Cis content determined by peak heights of the 740- and 1013-cm⁻¹ absorptions vs. cis content determined from integrated peak areas.

(i.e., peak heights) are therefore in error. This is demonstrated in Figure 6, which compares the values obtained by using integrated areas and absorbances. Differences between the two methods can be as high as 15%.

To corroborate the FTIR calibration, the 100 μm (PAC 1) and 22 μm (PAC 2) free-standing films were incrementally isomerized at 100 °C and examined by CP-MAS-NMR. The data for both films were essentially identical, and the evolution of the NMR spectra for the 100- μm film is shown in Figure 7. The resonance for ¹³C atoms associated with cis double bonds appears at 128 ppm vs. 137 ppm for those in trans double bonds.³⁸ The smaller peaks are due to spinning side bands, separated from the major resonances by the sample spinning rate (2.2–2.5 kHz). The initially weak trans signal grows with isomerization time while the cis signal diminishes. The relative areas of the cis and trans resonances were used to determine isomeric composition. Uncertainties range from 5% near the extremes to 2% near the 50–50 composition. The relationship of the composition determined by FTIR is compared to the composition determined by NMR in Figure 8. The results show a 1:1 correspondence within the experimental error limits. Therefore, FTIR and NMR can be

(38) Maricq, M. M.; Waugh, J. S.; MacDiarmid, A. G.; Shirakawa, H.; Heeger, A. J. *J. Am. Chem. Soc.* **1978**, *100*, 7729–7730.

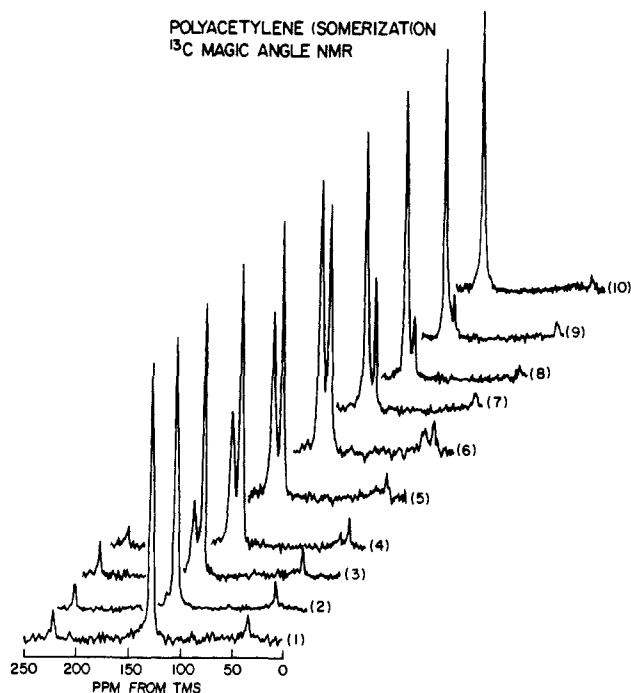


Figure 7. ^{13}C CP-MAS-NMR spectral evolution for the $100\ \mu\text{m}$ thick polyacetylene film (PAC 1). Spectrum No. (1) $25\ ^\circ\text{C}$, 1.5 days; (2) $25\ ^\circ\text{C}$, 9 days; (3) $25\ ^\circ\text{C}$, 11 days and $78\ ^\circ\text{C}$, 1 h; (4) $25\ ^\circ\text{C}$, 11 days and $78\ ^\circ\text{C}$, 1 h and $100\ ^\circ\text{C}$, 2 h; (5) $25\ ^\circ\text{C}$ 11 days and $78\ ^\circ\text{C}$, 1 h and $100\ ^\circ\text{C}$, 4 h; (6) $25\ ^\circ\text{C}$, 11 days and $78\ ^\circ\text{C}$, 1 h and $100\ ^\circ\text{C}$, 7.5 h; (7) $25\ ^\circ\text{C}$, 11 days and $78\ ^\circ\text{C}$, 1 h and $100\ ^\circ\text{C}$, 22.8 h; (8) $25\ ^\circ\text{C}$, 11 days and $78\ ^\circ\text{C}$, 1 h and $100\ ^\circ\text{C}$, 47 h; (9) $25\ ^\circ\text{C}$, 11 days and $78\ ^\circ\text{C}$, 1 h and $100\ ^\circ\text{C}$, 64 h; (10) $25\ ^\circ\text{C}$, 11 days and $78\ ^\circ\text{C}$, 1 h and $100\ ^\circ\text{C}$, 64 h and $200\ ^\circ\text{C}$, 21 min. The spectra are normalized to the larger of the two peaks. The smaller peaks at higher and lower fields are spinning side bands.

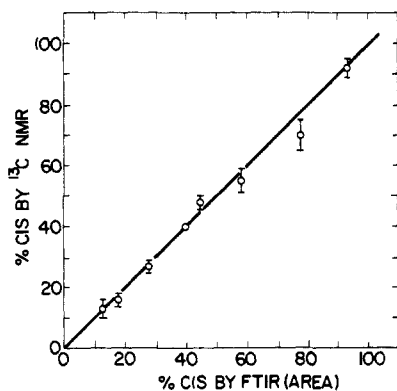


Figure 8. Isomeric composition of the $22\ \mu\text{m}$ polyacetylene film (PAC 2) as determined by CP-MAS-NMR vs. that determined by FTIR.

used in complementary fashion for isomeric composition determination—FTIR for thin samples whose low mass would disfavor use of NMR and the latter for thick samples whose high absorbance negates the utility of FTIR.

In order to ensure that the CP-MAS-NMR data are quantitative and that optimum signal intensities are obtained, proton relaxation behavior was measured as a function of isomerization. For mostly cis polyacetylene, $T_1 = 2\ \text{s}$ and $T_{1\rho} = 15\ \text{ms}$ (at $H_1 = 32\ \text{kHz}$), whereas for mostly trans polyacetylene $T_1 = 60\ \text{ms}$ and $T_{1\rho} = 7\ \text{ms}$. The T_1 response exhibits a single exponential recovery over the entire composition range because of the effect of spin diffusion. These data are consistent with the carbon signal being detected uniformly throughout the sample under our CP-MAS conditions. The decrease in relaxation times is attributed to the formation of unpaired spins during the isomerization.^{13,19,20}

III. Infrared Spectral Features. A detailed examination of the evolution of the features of the infrared spectra during the cis-trans isomerization provides information regarding the mechanism and

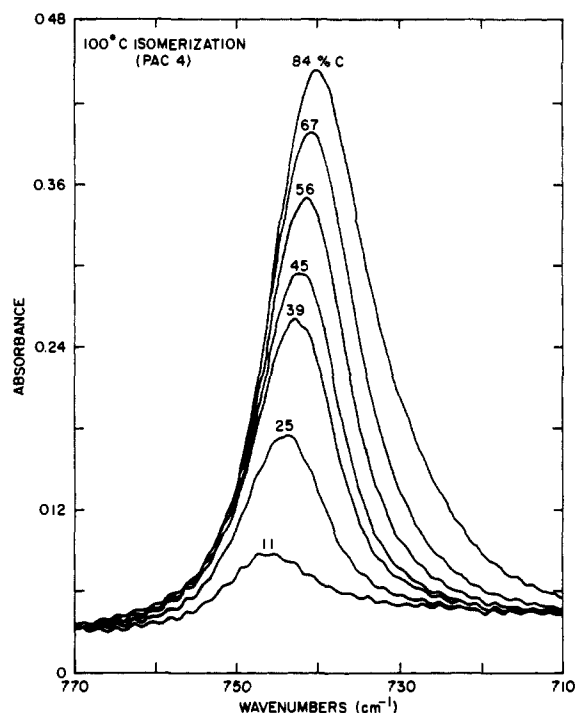


Figure 9. Evolution of 740-cm^{-1} absorption with time at $100\ ^\circ\text{C}$.

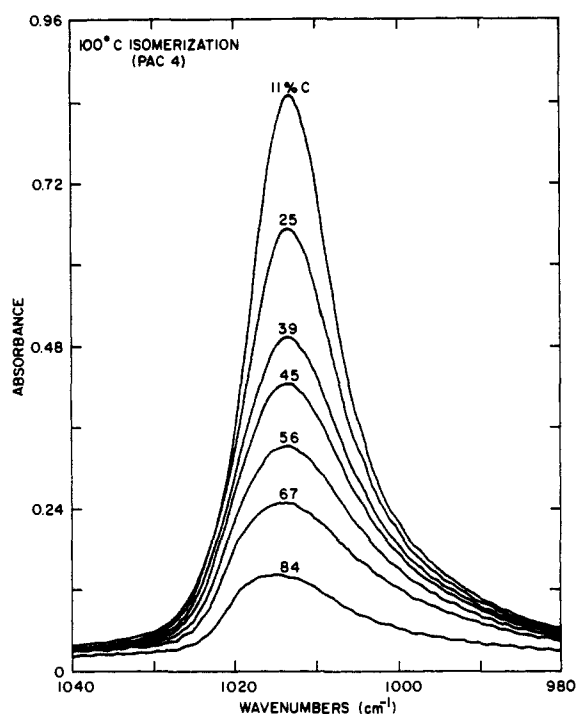


Figure 10. Evolution of 1013-cm^{-1} absorption with time at $100\ ^\circ\text{C}$.

the complexity of the transformation process. Small but measurable changes in both the shape and the position of the absorptions associated with the cis ($740\ \text{cm}^{-1}$) and trans ($1013\ \text{cm}^{-1}$) C-H out-of-plane modes occur during the isomerization (Figures 9 and 10). In contrast, the other identifiable cis ($1329\ \text{cm}^{-1}$ C-H in-plane deformation) and trans (3011-cm^{-1} C-H stretch) bands are well behaved, maintaining constant position, shape, and line width throughout the entire transformation.

The frequency of the absorption maxima and the line widths of the out-of-plane modes are a function of composition. The apparent maximum of the cis band shifts by more than six wavenumbers from $\sim 739\ \text{cm}^{-1}$ to $>745\ \text{cm}^{-1}$, while the $1013\ \text{cm}^{-1}$ trans band exhibits a much smaller (\sim one wavenumber) shift in the opposite direction (i.e., toward lower energies) as shown in

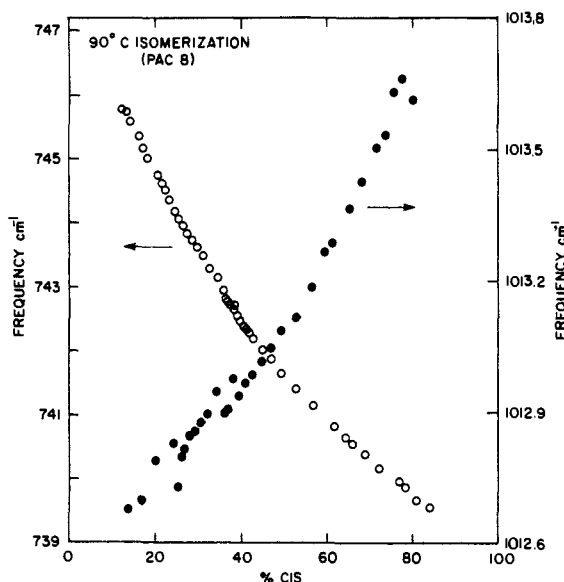


Figure 11. Frequency of the 740 (cis) and 1013-cm⁻¹ (trans) absorption maxima as a function of cis content during isomerization at 100 °C.

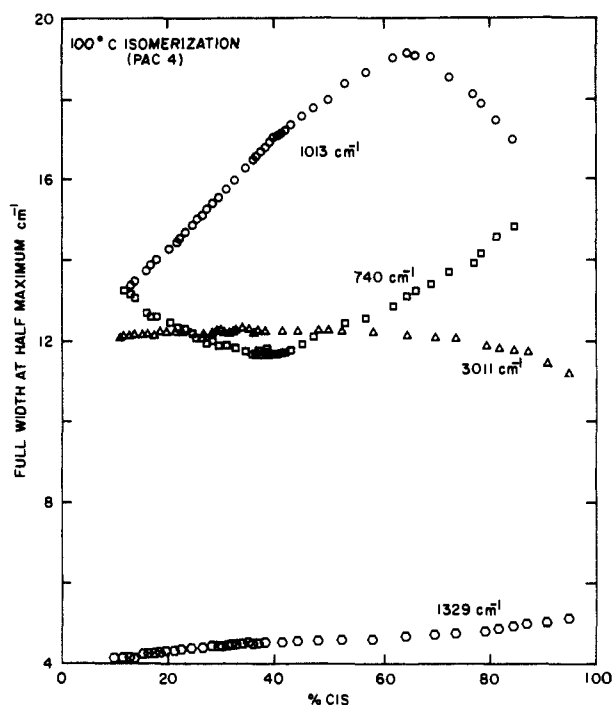


Figure 12. Full width at half maximum for the 740-, 1013-, 1329-, and 3011-cm⁻¹ absorptions as a function of cis content during isomerization at 100 °C.

Figure 11. In concert with these shifts are correlated changes in the shape of the bands as measured by the full width at half maximum (fwhm), shown in Figure 12. The trans (1013 cm⁻¹) band appears to broaden and then narrow while the cis (740 cm⁻¹) band follows the opposite trend. We propose that the 740- and 1013-cm⁻¹ absorptions are composite bands and that the apparent changes described above reflect changes in the intensities, and thus populations, of underlying modes. To a first approximation, this underlying structure can be resolved by analyzing the first and second derivatives of the spectra, shown in Figures 13 and 14. The minima in the second derivative of the 1013-cm⁻¹ trans absorption (Figure 14) suggest the presence of separate peaks at 1020 and 1013 cm⁻¹. Observed differences in the compositional dependence of the 1020- and 1013-cm⁻¹ bands would produce the apparent maximum in the fwhm vs. composition (Figure 12) and the change in slope of the frequency vs. composition plots (Figure 11). The first derivative of these spectra (Figure 13) shows that

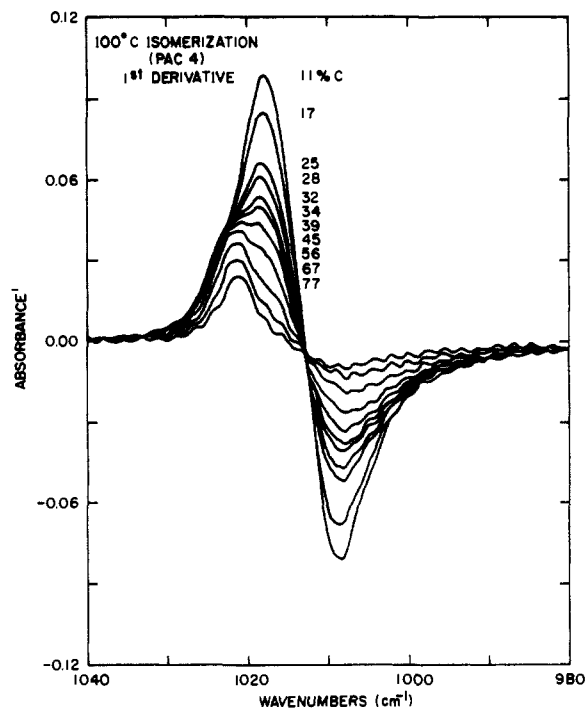


Figure 13. First derivative of the 1013-cm⁻¹ absorption as a function of percent cis isomer at 100 °C.

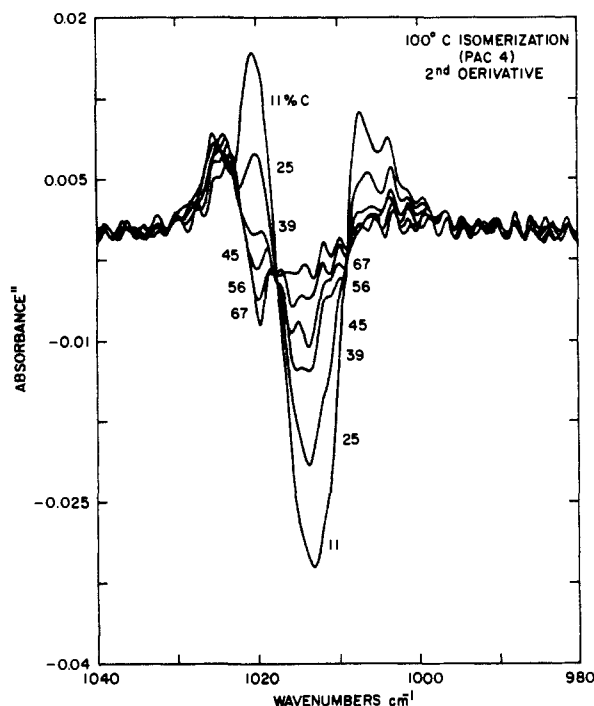


Figure 14. Second derivative of the 1013-cm⁻¹ absorption as a function of percent cis isomer at 100 °C.

the inflection associated with the higher energy peak at 1020 cm⁻¹ is not obscured by the dominant 1013-cm⁻¹ mode until the transformation is between half to two-thirds complete. While the derivatives of the 740-cm⁻¹ absorption are not able to resolve an underlying structure, the changes in the apparent band width (Figure 12) suggest the existence of overlapping modes.

This evidence for closely spaced bands is consistent with the trends predicted by Shirakawa's normal mode analysis of the sequence length dependence of the infrared spectra of polyacetylene C-H and C-D copolymers.³⁴ In that work, deuterated "defects" in a 10-unit segment of the same type of bond shifted the frequency of the protonated mode to progressively higher energies. While the calculations did not consider the presence

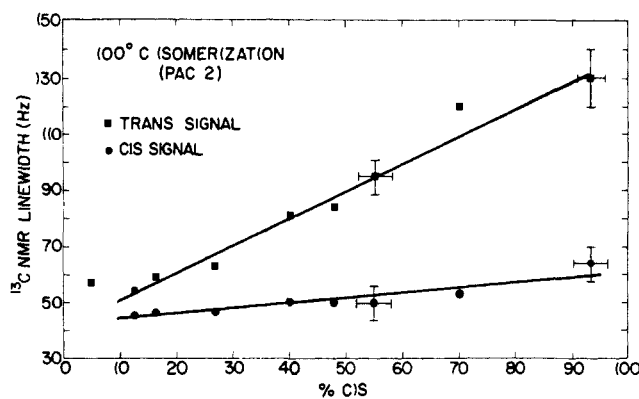


Figure 15. ^{13}C CP-MAS-NMR line widths for cis and trans resonances as a function of cis content for a 100 °C isomerization.

of trans bonds in a cis sequence, they do demonstrate that the frequency of a given bond is dependent on isomer block length. The gradual changes in band position and width observed in the present work imply that the creation of trans bonds occurs initially as isolated events and that longer run lengths only form later in the isomerization process. This conclusion is in agreement with the continuous changes in the unit cell parameters seen in the X-ray analysis of the isomerization process²⁴⁻²⁷ and with arguments presented below based upon CP-MAS-NMR line width data and IR analysis of the 1329 cm^{-1} band intensities.

IV. NMR Spectral Features. During isomerization the line widths of CP-MAS-NMR resonances associated with the cis and trans carbons of polyacetylene were measured as a function of the isomeric composition. These results are displayed in Figure 15. The line width of the cis signal varies very little during the isomerization, decreasing slightly with conversion from cis to trans. However, the trans signal's line width changes considerably during isomerization in linear response to the composition. This latter behavior is taken as evidence against a heterogeneous nucleated isomerization of the entire chains, which should produce a constant trans line width, but rather as evidence favoring a more random isomerization process. The trans line width is partly governed by the distribution of microstructural sequences. The approximate magnitude of this effect can be obtained by consideration of the chemical shifts of β -carotene and *cis*- β -carotene as model compounds. The chemical shift of the trans double bond carbon α to the central cis bond to *cis*- β -carotene is 126.8 ppm, which shifts downfield to 132.4 ppm in β -carotene, whose central double bond is trans.³⁹ This 5.6-ppm (127 Hz) shift is of the same order as the range of shifts measured for the polyacetylene trans peak. The cis peak, on the other hand, whose line width and position change little during isomerization, is apparently insensitive to microstructural sequencing.

The very broad trans line width early in the isomerization cannot be due to a distribution of cis (C) and trans (T) sequencing since initially only isolated pairs of trans units in TCT sequences should form (see below). Rather, the isomerization likely initiates in amorphous regions of polyacetylene, where differences in chain packing and bond angles contribute to a distribution of trans carbon environments. A similar mechanism has been proposed by Terao et al.⁴⁰ Even though our samples are typically highly crystalline,²⁴ if isomerization beings in amorphous regions, these regions can dominate the early trans line width.

The possibility of cross-linking during the synthesis of cis polyacetylene or during the isomerization to the trans isomer has been proposed.^{19-22,41,42} Such cross-links are assumed to arise from Diels-Alder reactions or from radical coupling reactions, both of which would generate sp^3 carbon atoms. The presence

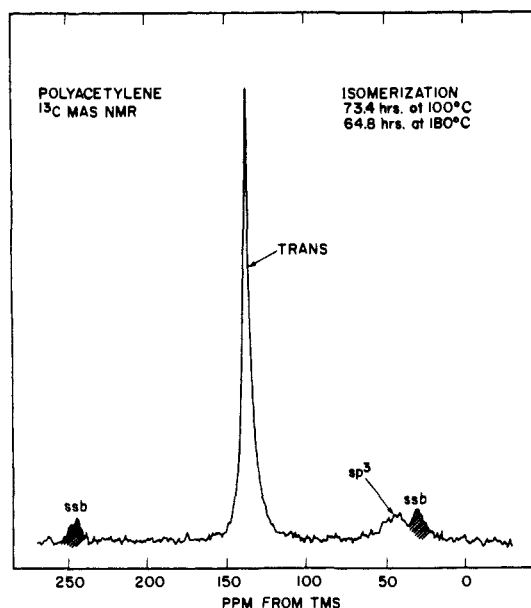


Figure 16. ^{13}C CP-MAS-NMR spectrum for a polyacetylene sample heated for 73.4 h at 100 °C followed by 64.8 h at 180 °C. Note the sp^3 signal at ~ 45 ppm.

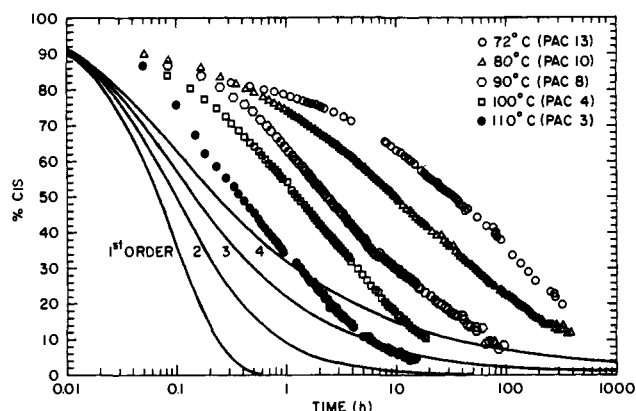


Figure 17. Cis content vs. log time for thin polyacetylene films on KBr at various temperatures and for theoretical first, second, and third order processes (from: Frost, A. A.; Pearson, R. G. *Kinetics and Mechanisms*, 2nd ed.; Wiley: New York, 1962; p 15, Figure 4).

of such sp^3 carbons would constitute breaks in the polyene conjugation and might be expected to influence the conductivity of the polymer. Other workers have indicated that NMR spectra of cis and trans "Shirakawa" polyacetylenes do not contain any evidence of sp^3 carbon atoms and estimate that, if present, they represent less than 2% of the sample.⁴³⁻⁴⁵ In our extensive studies of thermally isomerized samples, sp^3 carbon resonances were observed only in cases where the isomerization temperatures were high and the times long, e.g., 180 °C for 65 h. In Figure 16, such a spectrum is shown; the resonance at 40–50 ppm is attributed to sp^3 carbon atoms. In cases of the lower isomerization temperatures (or even short times at 200 °C) this resonance was not observed. Therefore, we concur that there are less than 2% sp^3 hybridized carbon atoms in trans polyacetylene prepared as described in the present work.

V. Kinetics and Mechanism of Isomerization. Most of the kinetic data were obtained from FTIR measurements of thin samples on KBr. Figure 17 shows the log-time dependence of the concentration of cis bonds during the 72, 80, 90, 100, and 110 °C isomerizations of the KBr supported films. In such a plot,

(39) Englert, G. *Helv. Chim. Acta* **1975**, *58*, 2367–2390.

(40) Terao, T.; Maeda, S.; Yamabe, T.; Akagi, K.; Shirakawa, H. *Chem. Phys. Lett.* **1984**, *103*, 347–351.

(41) Wegner, G. *Angew. Chem., Int. Ed. Engl.* **1981**, *20*, 361–381.

(42) White, C. T.; Brant, P.; Elert, M. L. *J. Phys. (Paris) Coll. C3* **1983**, *44*, 443–446.

(43) Bernier, P.; Schue, F.; Sledz, J.; Rolland, M.; Giral, L. *Chem. Scr.* **1981**, *17*, 151–152.

(44) Clarke, T. C.; Scott, J. C. *Solid State Commun.* **1982**, *41*, 389–391.

(45) Haberkorn, H.; Naarmann, H.; Penzien, K.; Schlag, J.; Simak, P. *Synth. Met.* **1982**, *5*, 51–71.

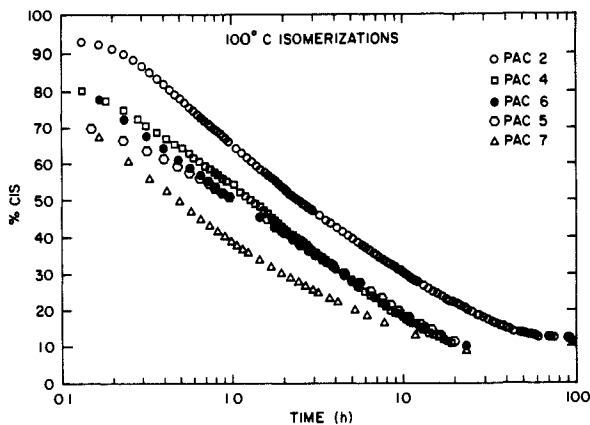


Figure 18. Cis content vs. log time for polyacetylene films at 100 °C.

differences in isomerization rates are manifested as a horizontal shift while the shape of the curve is characteristic of the kinetic process. Comparison of the shape of the experimental degree of conversion data over the entire isomerization with the solid curves (Figure 17), representing the calculated evolution of first, second, and third order reactions, shows that the isomerization is not a simple kinetic process of any order.

Different procedures for preparing polyacetylene films produce samples with, for the most part, reproducible but distinctly different isomerization rates. Figure 18 depicts the log time isomerization behavior at 100 °C for five separate films. Three of these films (PAC 4, 5, 6) were similarly prepared on KBr or glass substrates and reveal nearly identical isomerization responses. By comparison, the free standing film (PAC 2) isomerizes more slowly, and a film prepared with a pool of toluene surrounding the KBr substrate during polymerization (PAC 7) isomerizes more quickly. We believe that these differences arise from small differences in catalyst concentration or reaction temperature. Yet another sample (PAC 11, not plotted) isomerizes like the films prepared directly on KBr until the composition reaches 50% cis, at which point it isomerizes more slowly, like the free-standing film. It is our hypothesis that differences in isomerization rates are a manifestation of subtle differences in sample morphology not completely controllable synthetically or easily detected spectroscopically.

It was noted during this work that very thin films (<1 μm) have a very low as-prepared cis content (<50%). When attempts were made to prepare 2000-Å films transparent to visible light with the normal catalyst, the trans isomer was predominant. We believe that the initially formed material is amorphous in nature and that this disordered material comprises a larger portion of thin than of thick films. In comparison to crystalline regions, disordered regions have more free volume, thus reducing the activation barrier to bond rotation required for isomerization.⁴⁶ That the disordered regions may partially isomerize during polymerization or subsequent handling explains the high initial trans content of the thin films. In fact, even the thickest films measured by IR (~20 μm) had initial trans contents of 7–10%. The amorphous character of the initially formed polymer on the catalyst surface may be the result of the initially high active site concentration, which leads to a rapid polymerization rate⁴⁷ and tends to produce lower molecular weights and more structural disorder.⁴⁸ To produce highly (90%) cis films of ~2000-Å thickness it is therefore

(46) This might explain in part the large differences (6X) between the present isomerization rates and those of amorphous "Durham" polyacetylene (Edwards, J. H.; Feast, W. J.; Bott, D. C. *Polymer* **1984**, *25*, 395–398) as recently reported (Foot, P. J. S.; Calvert, P. D.; Ware, M. P.; Billingham, N. C.; Bott, D. C. *Polymer 85 Preprints*, Melbourne, Australia, pp 536–538; Foot, P. J. S.; Calvert, P. D.; Billingham, N. C.; Brown, C. S.; Walker, N. S.; James, D. T. *Polymer* **1986**, *27*, 448. Bott, D. C.; Brown, C. S.; Chai, C. K.; Walker, N. S.; Feast, W. J.; Foot, P. J. S.; Calvert, P. D.; Billingham, N. C.; Friend, R. H. *Synth. Met.* **1986**, *14*, 245.

(47) Aldissi, M.; Schue, F.; Giral, L.; Rolland, M. *Polymer* **1982**, *23*, 246–250.

(48) Eckhardt, H. *J. Chem. Phys.* **1983**, *79*, 2085–2086.

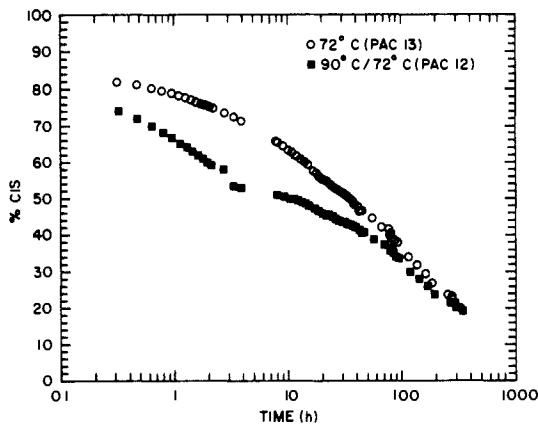


Figure 19. Cis content vs. log time for two samples, one isomerized at 72 °C and the other isomerized at 90 °C to 50% cis followed by isomerization at 72 °C.

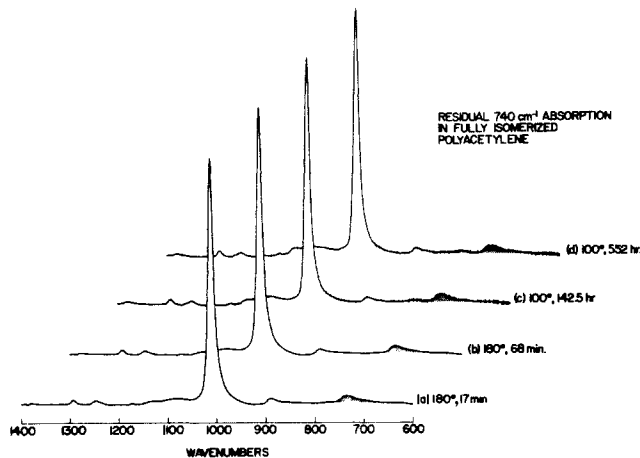


Figure 20. FTIR spectra of thin films of polyacetylene on KBr after treatment at 180 °C for 17 and 68 min and at 100 °C for 142.5 and 552 h showing the approximately constant residual 740-cm⁻¹ absorption.

Table II. Extended Time Results

T (°C)	time	residual 740 cm ⁻¹ as % cis
100	142 h	6.8
	552 h	6.7
	48 days	7.8
180	17 min	5.2
	68 min	5.6
	326 min	6.4
	26 h	6.8

necessary to utilize a dilute catalyst solution.⁴⁹

Because of the possibility of multiple consecutive concerted reaction processes in the isomerization there was concern that the rate might be dependent upon sample history. In order to test this possibility, two identical films on KBr were examined: the first (PAC 13) at 72 °C throughout the isomerization; the second (PAC 12) at 90 °C to ~50% cis and then 72 °C for the remainder of the isomerization. The time dependences of cis content for these isomerizations are compared in Figure 19. The 90 °C portion of the PAC 12 sample when shifted along the log time axis (by a factor of 7) reveals an identical shape to the 72 °C PAC 13 sample. Thus, although the rates are different, the processes responsible for the isomerization are identical, independent of temperature. Furthermore, the 72 °C portion of PAC 12 superimposes with the PAC 13 curve after adding a constant 30 h to the PAC 12 data to account for the fact that the 90 °C history

(49) Chung, T. C.; Feldblum, A.; Heeger, A. J.; MacDiarmid, A. G. *J. Chem. Phys.* **1981**, *74*, 5504–5507.

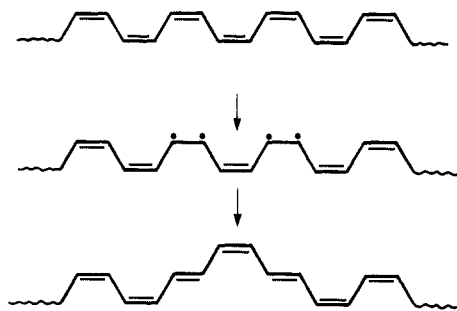


Figure 21. Preferred initial isomerization pathway involving a crankshaft rotation about two simultaneously formed biradicals to convert a CCC to a TCT triad sequence.

of PAC 12 advanced it by 30 h relative to PAC 13. Despite the different thermal histories, at 72 °C both samples obey the same kinetics, i.e., the same rates and presumably the same mechanisms. It appears that thermal history does not affect the kinetics of isomerization, at least in this temperature region.

Consistent with the observations of Ito, Shirakawa, and Ikeda,⁸ the 740-cm⁻¹ absorption never fully disappeared in any sample, even at 180 °C. Representative spectra are shown in Figure 20. Table II displays the observed end points for a number of temperatures and times. Trans polyacetylene samples prepared by isomerization of "Shirakawa" material contain 5–7% remnant cis isomer. This fact must be accommodated by any mechanistic proposals and kinetic rate expressions. Elsewhere^{32,33} we proposed that the 740-cm⁻¹ absorption is due to the presence of either cis-transoid or trans-cisoid linkages or both. The quantitative trapping of these units by maleic anhydride⁵⁰ indicates the presence of trans-cisoid units or their involvement in an equilibrium with the cis-transoid form.

The mechanism of isomerization is believed to involve a number of processes, the easiest of which is the triad conversion, CCC → TCT (Figure 21), via a crankshaft rotation about two simultaneously formed biradicals.⁵¹ Such a mechanism is favored because only local displacement of two carbon atoms is required. In contrast, isomerization of a single cis unit to trans is less likely since it involves either a major displacement by the entire polymer chain or small conformational rearrangements by many bonds surrounding the transforming site. Similarly, other triad process, CCT ⇌ TCC, can rearrange sequencing within a polymer chain to allow the above "easy" process to further transform cis to trans bonds. Tetrad and higher order processes, although less favored, are believed to contribute to the latter stages of the isomerization.

In order to examine these mechanisms, the behavior of the 1329- and 3011-cm⁻¹ bands was investigated in some detail. The 1329-cm⁻¹ cis in-plane C–H deformation is of particular interest since this band has been attributed to an extended cis mode.¹⁰ A log–log plot of the 1329-cm⁻¹ band vs. percent cis as determined by the 740/1013 cm⁻¹ out-of-plane local modes for a number of polyacetylene samples is shown in Figure 22. The log–log plot is a useful presentation since the shape of the curves is independent of film thickness and band extinction coefficients, which only result in linear data offsets. It is noteworthy that for all of the samples a nearly linear log–log plot with a slope of ~1.5 is obtained over a large portion of the isomerization. Extrapolation to $t = 0$ gives an initial linear relationship with a slope of 1.5. That is, for every two cis bonds which convert to trans via a CCC → TCT transformation, the 1329 cm⁻¹ band loses three cis units of intensity. One obvious interpretation for this observation is that the 1329 cm⁻¹ band does not detect the isolated cis bond created by this triad process but does detect all other cis units equally. With this assumption regarding the 1329 cm⁻¹ band, modeling of the isomerization as a random process and allowing only triad conversions gives the predicted dependence of the 1329 cm⁻¹ band

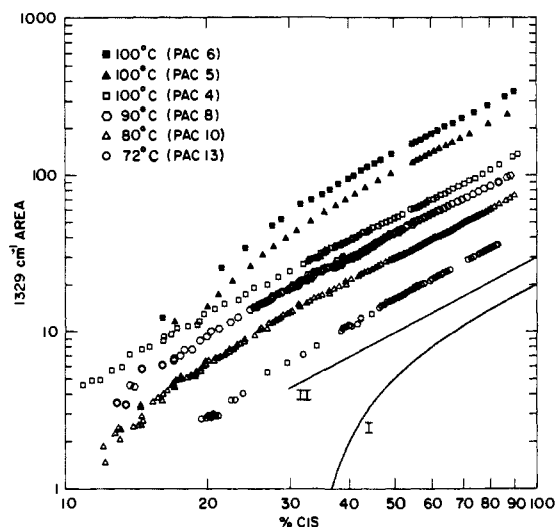


Figure 22. log–log plot of the 1329-cm⁻¹ cis in-plane deformation band area (in arbitrary units) vs. cis content for a number of polyacetylene isomerizations. For clarity, the PAC 10 and PAC 13 band areas have been divided by 2 and 4, respectively. Curves I and II are predicted behaviors assuming random triad processes but with different assumptions regarding the nature of the 1329-cm⁻¹ band (see text).

on isomer composition shown by curve I in Figure 22.

The analysis was performed by simulating the isomerization of a polyacetylene chain of 100 cis double bonds. Each successive isomerization site was selected by the random number generator of the Hewlett Packard Stat Pac software for an HP-67 calculator. At this randomly determined site, CCC → TCT and CCT ⇌ TCC triad processes were permitted to occur, and after each step the 1329-cm⁻¹ band intensity was recalculated. This procedure was repeated several times and the results averaged to generate curve I in Figure 22. The same result was obtained when all three triad processes were allowed to occur equally or when CCC → TCT processes were always required to go to completion before other processes could occur. This model gives a reasonable fit only to the early time behavior of the isomerization; for later times the experimental 1329-cm⁻¹ area data fall off significantly more slowly than the predicted curve.

A better fit can be obtained assuming that the contribution of a cis bond to the 1329-cm⁻¹ band intensity diminishes by 1/4 for each neighboring trans unit. That is, an isolated cis bond only contributes half the intensity that the central cis in a CCC sequence contributes to the 1329-cm⁻¹ band intensity. With this assumption, modeling of the isomerization as above results in curve II in Figure 22. This analysis fits the experimental data for all samples studied over the initial 70% of the isomerization. Furthermore, the random nature of the isomerization assumed by this model is consistent with the above-mentioned NMR line width and IR band position data. The cis bonds left after all triad processes are exhausted can only isomerize by less favored higher order coordinated processes. Such coordinated processes require specific sequences; hence there is a statistical limit. Because of the high activation energy to convert isolated cis bonds all polyacetylenes have residual cis isomer, as discussed above.

In contrast to the 1329-cm⁻¹ band, the 3011-cm⁻¹ band shows a linear response with trans content for all samples studied. These data, shown in Figure 23, are consistent with the 3011-cm⁻¹ band assignment to a local trans mode. Systematic errors in integrating this band at low trans contents (because of a neighboring cis band at ~3040 cm⁻¹) appear to be responsible for the data not passing through the origin.

Conclusions

The experimental results reported here lead to the following conclusions regarding the isomerization of Shirakawa-type polyacetylene. Though it is possible to reproducibly prepare thin films of polyacetylene, the isomerization rate is sensitive to subtleties in the synthetic technique. It is suggested that varying

(50) Gibson, H. W.; Weagley, R. J.; Mosher, R. A.; Kaplan, S.; Prest, W. M., Jr.; Epstein, A. J. *Br. Polym. J.* **1986**, *18*, 115–119.

(51) Yamabe, T.; Akagi, K.; Ohzeki, F.; Fukui, K. *J. Phys. Chem.* **1982**, *43*, 577–581.

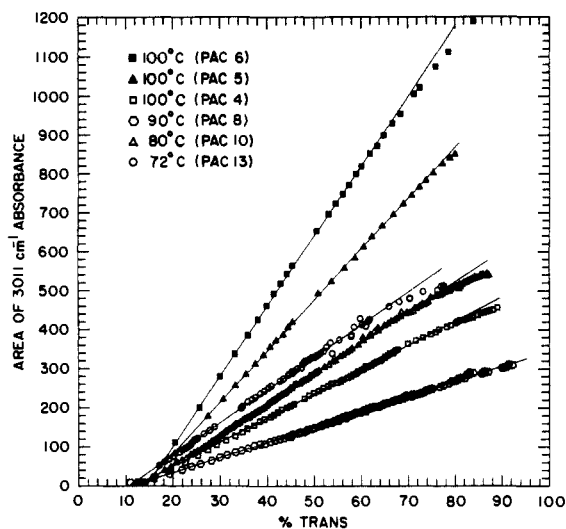


Figure 23. 3011-cm⁻¹ trans CH stretch band area (in arbitrary units) vs. cis content for a number of polyacetylene isomerizations.

amounts of amorphous and crystalline morphology are produced and that the isomerization rate depends upon the distribution of local fluctuations in morphology. The breadth of the NMR trans peak and IR determination of initial isomeric content with film thickness support the conclusion that the isomerization initiates in disordered regions. The kinetics of isomerization between 72 and 110 °C have been determined; the data are not accommodated by simple order kinetics. Evidence is presented that the isomerization proceeds as random sequential events and is not a heterogeneous nucleation of isomerization of entire chains. The arguments are based on the continuous changes in line width and position of the IR out-of-plane deformation bands, the continuous changes in intensities of the underlying modes of the trans out-of-plane deformation band, and the continuous decrease in the NMR trans peak line width. Furthermore, behavior of the 1329-cm⁻¹ cis in-plane deformation band is consistent with most of the isomerization proceeding as random triad "easy" processes, CCC → TCT, followed by successive CCT ⇌ TCC processes, which facilitate additional "easy" conversions. Even though isomerization rates may vary, these mechanisms prevail for all of the samples studied, independent of sample preparation, history, and isomerization temperature. Because of the difficulty in the solid state of converting isolated cis bonds, all samples examined, regardless of the time or temperature of isomerization, contain 5–7% remnant 740-cm⁻¹ absorption. Sp³ carbon atoms are not detected in any cases, except for long times at high temperatures (65 h, 200 °C).

Experimental Section

Sample Preparation. All synthesis and handling operations were carried out in an oxygen- and water-free (<0.8 ppm, <0.3 ppm, respectively) glovebox or vacuum line. Catalyst preparation, acetylene purification, and other general procedures were as reported previously.² New KBr discs (25 mm diameter, 4 mm thick) obtained from Janos Optical Corp. were washed with dry, degassed toluene in the glovebox and dried prior to use. Polyacetylene samples synthesized by three slightly different procedures were used in this study. Thin films deposited directly on KBr and glass discs were prepared by using a modified Shirakawa technique (below). One of the thin films (PAC 7) was prepared by a slight modification, namely the presence of a "pool" of dry degassed toluene sur-

rounding the KBr substrate supported by a glass disc. Thicker (up to 100 μm) free-standing films were prepared in the "normal" way by using the standard Shirakawa catalyst.²

In a typical experiment to prepare films deposited on substrates the Shirakawa catalyst (0.92M Et₃Al/0.23M Ti(OBu-n)₄ in toluene) was aged for 0.5 h at room temperature, degassed,² transferred back into the glovebox (total aging: 1 h at 25 °C), and applied by means of a syringe to the substrate (seven drops from a 16 gauge needle for a 25 mm diameter disc) in a cylindrical flat-bottomed reactor. The reactor vessel had two arms, one for the acetylene supply and the other for the vacuum system. After attachment to the vacuum line the argon was removed by brief (60 s) pumping while cooling the lower half of the reactor with liquid nitrogen. Following equilibration at -78 °C (dry ice/acetone) a preset pressure (~450 Torr) of purified acetylene gas was admitted to the reactor for 30–40 s. The reactor was isolated from the acetylene supply and pumped out by the rough vacuum system for several minutes at -78 °C and then pumped out by the high vacuum system for 15 min at -78 °C and for 10 min while warming up. The reactor was then transferred to the glovebox where the films were washed exhaustively with purified toluene and/or pentane. By this technique it was possible to prepare reproducible films of uniform thickness (as evidenced by the SEM in Figure 2). Preparation of one sample on a glass disc (PAC 6) followed by flotation and transfer of the washed film onto a KBr disc showed that the substrate for the film synthesis had minimal, if any, effect on the isomerization rate.

Isomerization of samples (22 and 100 μm thick) for NMR study was carried out in evacuated (10⁻⁵ Torr) sealed glass ampules by suspension in refluxing solvent vapors.

FTIR Spectroscopy. FTIR data were obtained on a Digilab FTS-15C instrument run at 1-cm⁻¹ resolution. Freshly prepared samples on KBr were contained in a heated cell (Beckman RIIC) sealed under argon. The cell was placed in the IR sample compartment, which was continuously purged with dry nitrogen (from a high-pressure liquid-nitrogen tank). A calibrated thermocouple was situated ~2 mm from the surface of the film inside the cell. The temperature was manually controlled to ±1 °C by means of a Variac connected to the heater. Typically, 64 scans were averaged for each spectrum. Spectra were recorded every 2–5 min at the start of the isomerization and at progressively longer intervals as isomerization proceeded. From 50 to 200 spectra were recorded during each run. The various peaks were integrated by establishing base lines between points on each side of the absorption peaks. These points were chosen by examination of a range of spectra from a variety of samples so as to include the entire peak of interest but exclude neighboring peaks. The base line points were as follows: for the 740-cm⁻¹ band, 650 and 800 cm⁻¹; for the 1013-cm⁻¹ band, 940 and 1055 cm⁻¹; for the 1329-cm⁻¹ band, 1310 and 1340 cm⁻¹; and for the 3011-cm⁻¹ band, 2980 and 3040 cm⁻¹.

NMR Spectroscopy. ¹³C NMR spectra were obtained at ambient temperature with a Bruker CXP spectrometer at 22.63 MHz. Proton enhanced cross polarization used a 1 ms contact time, high power ($H_1 = 12$ G) proton decoupling, and magic angle spinning at 2.2–2.5 kHz. The spectra in Figure 7 (PAC 1) were obtained with a recycle time of 1 s, whereas the quantitative data used for Figure 8 (PAC 2) used recycle times of five times the measured proton T_1 but never less than 1 s. Cis/trans compositions based on ¹³C spectra of both PAC 1 and PAC 2 data were always within 5 percentage points of one another for identical isomerization times. No T_1 distortion occurs since proton spin diffusion is operative. Samples were contained in a sealed (threaded) Kel-F (3M Co.) rotor, which also contained some KBr to facilitate adjustment of the magic angle. Spinning in a Beams type assembly was accomplished by a stream of dry nitrogen gas which served to purge the sample compartment. Sample sizes were ~15 mg. Typically, 50 000 scans were averaged to give a signal-to-noise ratio of 30–50:1 for the larger peak.

Acknowledgment. The authors acknowledge helpful discussions with A. J. Epstein and H. Rommelmann. Scanning electron microscopic examination, e.g., Figure 2, was carried out by H. Rommelmann, to whom we express our gratitude.